High-frequency Characterization of the Physicochemical Parameters of Cook Inlet, Alaska

Principal Investigator: Amanda Kelley

College of Fisheries and Ocean Sciences, University of Alaska Fairbanks

March 2021

Final Report

OCS Study BOEM 2021-018

Contact Information:

uaf-cmi@alaska.edu
Phone: 907.474.6782
https://www.uaf.edu/cfos/research/cmi

This study was funded by the U.S. Department of the Interior, Bureau of Ocean Energy Management (BOEM) Alaska OCS Region (Cooperative Agreement M17AC00011) and the University of Alaska Fairbanks. This report is available from the Coastal Marine Institute and online at https://www.boem.gov/newsroom/library/scientific-and-technical-publications.

The views and conclusions contained in this document are those of the authors and should not be interpreted as representing the opinions or policies of the U.S. Government. Mention of trade names or commercial products does not constitute their endorsement by the U.S. Government.

Table of Contents

List of Figures iv
List of Tables iv
Abstract v
Introduction 1
Methods 3
Sensor arrays and site selection 3
Sensor calibration: reference sample collection and analytical measurements 4
Sensor uncertainty and overall accuracy 5
Statistical analyses 6
Results 6
Annual time-series analysis 6
Seasonal time-series analysis 8
Power spectral density analysis 10
Uncertainty estimates 11
Discussion 11
Conclusion 13
Acknowledgments 13
Study products 13
References 14

List of Figures

Figure 1. pH sensor deployment sites within Kachemak Bay, Alaska 3

Figure 2. PI Kelley deploying a SeapHOx sensor on a pier piling in Seldovia, Alaska..... 4

Figure 3. UAF student Noah Khalsa filling sample bottles with recently collected reference seawater..... 5

Figure 4. UAF students Alta Dean and Ryan Kramer measuring pH using the spectrophotometer..... 5

Figure 5. Homer time-series of pH, temperature, salinity, and dissolved oxygen for the entire deployment period, 7/2/18 to 8/4/2019..... 7

Figure 6. Seldovia time-series of pH, temperature, salinity, and dissolved oxygen for the entire deployment period, 10/7/17 to 8/4/2019..... 7

Figure 7. Homer summertime temperature-salinity scatterplot with a quadratic fit line..... 8

Figure 8. Seldovia summertime temperature-salinity scatterplot with a quadratic fit line..... 9

Figure 9. Scatterplot of temperature and salinity at Seldovia during wintertime 9

Figure 10. Scatterplot of temperature and salinity at Homer during wintertime 10

Figure 11. Homer summer Power Spectral Density (PSD) plot 10

Figure 12. Seldovia summer Power Spectral Density (PSD) plot 11

List of Tables

Table 1. Summary statistics of measured parameters, 7/2/2018 – 8/2/2019. 8

Abstract

Little is known about how ocean acidification (OA), a decline in ocean pH due to the absorption of anthropogenic carbon dioxide by the world's oceans, affects the nearshore environment. Nearshore ecosystems help to protect the coastline and provide important habitats for marine animals. Because these ecosystems are highly dynamic and complex, it has been challenging to accurately monitor ocean chemistry changes in coastal waters, especially along Alaska's vast coastlines. A dearth of baseline ocean pH data makes it difficult to determine the human-caused and natural influences on ocean pH variability. Measuring OA is increasingly essential to understand how marine ecosystems will respond to global ocean change. Advances in pH sensor technology have led to increased OA monitoring along the west coast of the United States. Evidence suggests that OA threatens marine species vital to Alaska's fisheries, and addressing this challenge on a local scale is a concern for policymakers and managers in the state. The goal of the project was to deploy oceanographic sensors to measure pH, temperature, conductivity (calculate salinity), and oxygen concentrations in high-frequency (hourly) to improve our understanding of nearshore carbonate chemistry and inform biological studies investigating aspects of OA tolerance and local adaptation in Alaska.

Introduction

Human activities have contributed to the notable global-scale changes occurring in the earth's physical, chemical, and biological processes (Waters et al. 2016). A byproduct of human activities, carbon dioxide (CO_2), a greenhouse gas, is largely responsible for observed climatic shifts. CO_2 released into the atmosphere has directly modulated an increase in atmospheric temperature (IPCC 2013) and, for marine ecosystems, these shifts manifest as an increase in seawater temperature and a decrease in ocean pH due to absorption of atmospheric CO_2 by the world's oceans, a process termed ocean acidification (OA). The development of stable and accurate pH sensors (Martz et al. 2010) has enabled coastal pH studies to demonstrate the complexity of natural nearshore dynamics, both spatially and temporally (Kapsenberg et al. 2015; Kapsenberg and Hofmann 2016). Observations of high pH variability confound our understanding of organisms' sensitivity to OA and complicate reliable detection of anthropogenic signals in coastal pH seascapes. Other abiotic factors influence the frequency and amplitude of pH variability. Increasing freshwater discharge, driven by climate change, accentuates and accelerates ocean acidification (Evans et al. 2014). These human-driven environmental changes are expected to continue and intensify if atmospheric CO_2 concentrations, as predicted, continue to increase (IPCC 2013). The impacts of anthropogenic CO_2 are already evident as ocean pH continues to decrease and ocean temperatures continue to rise (IPCC 2013). The physical and chemical changes highlighted above raise numerous questions about the long-term persistence and sustainability of marine ecosystems.

From a geochemical perspective, Alaskan coastal waters have an increased risk of acidification due to the ability of cold subarctic and arctic water to hold more CO_2, which shifts the total dissolved inorganic carbon (DIC) species' distribution and acid-base equilibrium. Alaskan coastal waters are highly productive in the boreal spring and summer. The resulting organic carbon remineralization from the demise of this production markedly increases DIC, leading to autumn acidification events (Fabry et al. 2009; Reisdorph and Mathis 2015). The few published studies that characterize the carbonate system in Alaska's marine environments (e.g., Bates et al. 2009; Reisdorph and Mathis 2014) have identified episodic periods of acidification and undersaturation in ecologically important habitats, underscoring the need to establish baseline data sets for tracking future ocean changes.

The pH of Alaska waters and elsewhere have decreased 0.1 units since the Industrial Revolution, and we anticipate a further decrease of another 0.4 units by the end of the century (IPCC 2013). This change in ocean pH poses a challenge to the marine environment across all levels of biological organization, from cellular-level responses to ecosystem dynamics (Somero et al. 2016). OA reduces the carbonate saturation state of seawater, making it energetically costly for organisms to produce calcium carbonate (Waldbusser et al. 2015), which is precipitated by many Alaskan marine species, including phytoplankton and invertebrates such as pteropods, oysters, bivalves, crabs, and sea urchins. OA can also alter organisms' physiology and growth, particularly in their early life stages, negatively affecting both fish and shellfish recruitment, thus

modifying ecosystem structure and function (Kroeker et al. 2013). In turn, variation in abundance and performance of prey fish and invertebrates has important consequences for top consumers in marine systems, including marine birds and mammals (Waldeck and Larsson 2013).

The specific threats of acidification will disproportionately affect coastal communities and economies in Alaskan waters sooner than other parts of the USA via deleterious effects on shellfish and fisheries (Ekstrom et al. 2015). Many of the commercial fisheries in Alaska rely on healthy nearshore habitats, which serve as nursery grounds for species such as salmon and herring (Cooney et al. 2001) and year-round habitat for many species of shellfish, gastropods, and echinoderms (Iken et al. 2010; Pohle et al. 2011; Miloslavich et al. 2013). Very little is known regarding coastal pH dynamics in Alaska's nearshore habitats. To date, there are no published studies documenting high-frequency nearshore pH dynamics for the state of Alaska. Evans et al. (2015) characterized high-frequency (hourly) pH time-series data at the Alutiiq Pride Shellfish Hatchery in Seward, Alaska; however, they collected only seven months of data, too little to detangle seasonal effects on pH dynamics on an annual timescale. Furthermore, the facility's seawater intake is in 75 m of water ~ 500 m from shore in Resurrection Bay, so it would not capture specific physical and biological processes that nearshore environments exhibit.

Alaskan waters, and the Gulf of Alaska (GoA), in particular, are experiencing unprecedented changes related to anthropogenic climate forcing (Walsh et al. 2018). "The Blob," an episode of extreme ocean warming, lingered in the GoA in 2014, driving alterations to the marine ecosystem, including species range shifts and closures of commercially important species (Cavole et al. 2016; Litzow et al. 2020). Ocean warming is, however, only one of the byproducts of anthropogenic CO_2; OA is the other (Doney et al. 2009). Alaska benefits from a five-billion-dollar a year fisheries industry that is highly dependent on the continued health and productivity of Alaska's marine resources, and state leaders recognize the importance of OA research in protecting this resource. Alaskan senator Lisa Murkowski recently proposed a new senate bill titled "the Coastal Communities Ocean Acidification Act" to address the threat of OA in Alaska. Political action at this high level underscores the need for information regarding Alaska's vulnerability to OA.

Due to its cold, nutrient-rich waters, the GoA is categorized as a Class I productive ecosystem harboring more than 300 grams of carbon per square meter per year (Hogan 2011). This unusually high productivity supports a complex food web that sustains Alaska's robust fisheries industry and culturally important subsistence harvesting of marine resources. A recent analysis identified the larger GoA as highly vulnerable to OA in a risk assessment model based on substance fishing, low industry diversity, and economic dependence on fishery harvests (Mathis et al. 2014). Nearshore areas in the GoA are particularly vulnerable to OA due to the presence of seasonal, large-scale glacial runoff of low-alkalinity freshwater and the upwelling of waters from deep GoA that are CO_2-rich and undersaturated with respect to aragonite ($\Omega arag < 1$; Evans et al. 2013; 2014).

The study site, Kachemak Bay, Alaska, served as an ideal location for high-latitude ocean change research due to its proximity to Homer, a community that community relies heavily on commercial and subsistence harvest of marine resources. Kachemak Bay (KB) is an iconic example of Alaska's amply productive and diverse high-latitude coastal waters that will likely be vulnerable to OA in the near future. KB lies in the northern GoA (60˚N 151˚W) and has an area of 1,500 km² and 540 km coastline. The bay is a large, shallow estuary divided into an inner and outer bay at the Homer Spit (Figure 1). KB hosts a broad diversity of macrophytes, echinoderms, gastropods, and decapods, ranking it as one of the most diverse estuarine systems in the world (Iken et al. 2010; Konar et al. 2010; Pohle et al. 2011; Miloslavich et al. 2013). The bay's benthic communities include 242 invertebrate species (including 108 mollusks and 78 polychaetes) and 237 macroalgal species (Konar and Iken 2005).

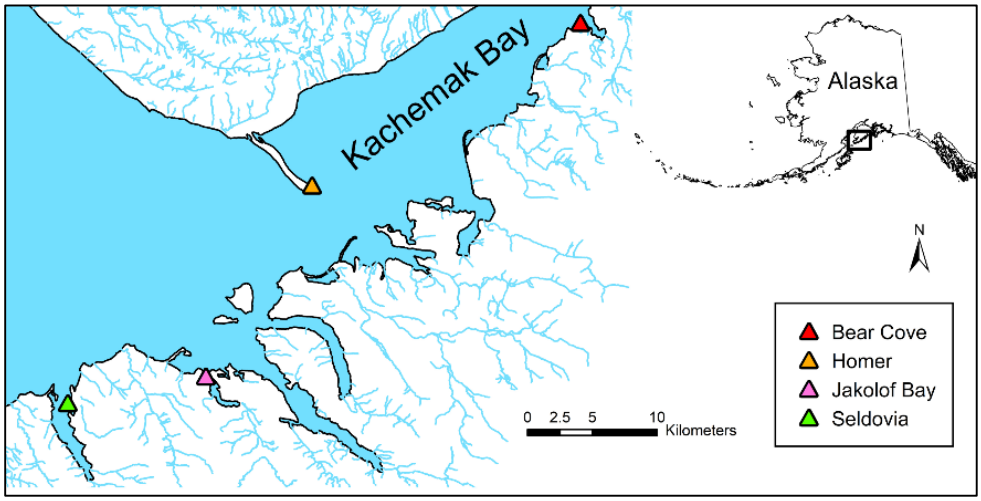

Figure 1. pH sensor deployment sites within Kachemak Bay, Alaska. Seldovia (green triangle) and Homer (orange triangle).

The streams feeding the estuary serve as nursery grounds for coho salmon, sockeye salmon, and pink salmon (Neher et al. 2014), which further illustrates the broad taxonomic diversity of KB. Ocean drifters in KB and lower Cook Inlet indicate a single eddy at the KB entrance and support a counterclockwise circulation theory within the bay. Key drivers of this circulation are freshwater discharge from surrounding glaciers and terrestrial freshwater riverine input. Oceanic water from the Alaska Coastal Current enters the bay from the southwest and, as the water moves counterclockwise, it is infused with glacial and river water that freshen it as it exits the bay. Therefore, KB provides an excellent study system to determine the biological and physical drivers of pH variability in a high-latitude marine ecosystem within the BOEM study region of lower Cook Inlet.

Methods

Sensor arrays and site selection

The sites chosen for sensor deployment in KB, Homer (HOM), and Seldovia (SEL) (Figure 1) are along a freshwater gradient within the bay and were anticipated to have different pH

variability due to the influence of freshwater on the carbonate system. Furthermore, biological productivity, from organismal respiration and primary productivity from phytoplankton and macroalgae, varies from site to site. At each site, a sensor array including a Sea-Bird SeapHOx sensor (which combines the SeaFET V2 pH sensor with the SBE 37-SMP-ODO MicroCAT CTD and DO sensors, measuring pH, temperature, salinity, and dissolved oxygen) and a PAR sensor was deployed roughly 7 m from the surface and secured to a pier piling (Figure 2). Each SeapHOx was outfitted with a mesh copper cap over the electrodes to prevent biofouling. Instrument sampling occurred every three hours continually for all instruments. This sampling regime allowed for short-term analysis of variability and includes both the tidal and photoperiod influence on pH. The SEL sensor array was deployed on October 7, 2017, and recovered on August 16, 2019. The HOM array was deployed July 2, 2018, and retrieved August 16, 2019. Reference seawater sample collection occurred every 4–6 months, weather permitting.

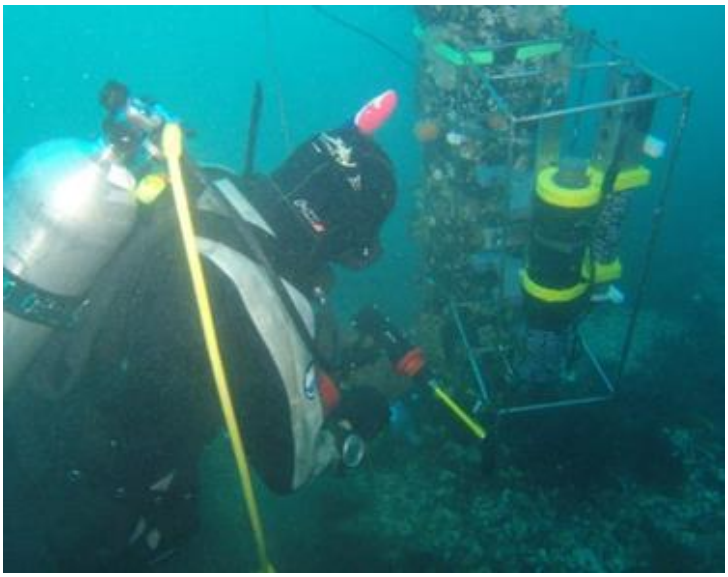

Figure 2. PI Kelley deploying a SeapHOx sensor on a pier piling in Seldovia, Alaska.

Sensor calibration: reference sample collection and analytical measurements

Discrete water samples were collected for pH calibration using a Niskin bottle fixed proximal to each sensor array (Figure 2). Collections occurred within 30 seconds of the instrument sampling time. Samples were stored in glass bottles (Figure 3), fixed immediately with 200 µl saturated mercuric chloride, and held in a refrigerator at ~ 4°C. The pH of each sample was measured at 25°C (spectrophotometric method, SOP 6b, Dickson et al. 2007; using meta-cresol purple from Acros, batch # 30AXM-QN) (Figure 4). A dye impurity correction factor (Douglas and Byrne 2017) was applied to the final calculation of pH_T (total scale). Total alkalinity (TA) was measured using open-cell titration (A_T, SOP 3b; Dickson et al. 2007). A YSI 3100 conductivity instrument was used to measure salinity, and temperature was measured at the time of collection using a digital thermometer (Omega, HH81A). pH_T *in situ* was calculated with CO2Calc (Robbins et al. 2010), using constants from Mehrbach et al. (1973) refit by Dickson and Millero

(1987), with input parameters spectrophotometric pH (25°C) and TA. Using the calculated pH_T from the discrete bottle samples, electrode-specific single-point calibration coefficients were applied to each pH dataset (Bresnahan et al. 2014; Miller et al. 2018). Each calibration/reference sample was collected in duplicate, and pH_T from each replicate bottle sample was measured in duplicate for analytical precision.

Figure 3. UAF student Noah Khalsa filling sample bottles with recently collected reference seawater.

Figure 4. UAF students Alta Dean and Ryan Kramer measuring pH using the spectrophotometer.

Sensor uncertainty and overall accuracy

Analytical uncertainty of spectrophotometric measurements with m-cresol was examined via duplicate analytic precision using Certified Reference Material (CRM: Batch 172, A.G., Dickson, Scripps Institute of Oceanography) based on the calculated pH of the CRM given the input parameters of TA, DIC, salinity, and measurement temperature. pH uncertainty was

estimated for each time-series by calculating the absolute value of the difference between the reported calibrated SeaFET value and the laboratory-measured *in situ* pH value of the reference sample taken throughout the deployment period.

Statistical analyses

A Student's t-test was carried out to compare oceanographic variables across sites for the annual time-series, from 7/2/2018 – 8/2/2019, at both sites. The last two weeks of the HOM and SEL time-series were removed for ease of comparison. The effect of seasonality on physical and biological variability (salinity, temperature, oxygen concentration) can limit these factors' correlation to pH variability. To better ascertain the relationship between pH and the other measurement variables, the time-series for each site was divided into summer (5/1/19 – 8/4/19) and winter (10/1/18 – 3/31/19) periods (Miller et al. 2021). Relationships between pH and salinity, oxygen concentration, and temperature are seldom linear and were correlated by applying a quadratic fit for the summer period. A power spectral density (PSD) analysis of pH was performed using the pwelch function to determine the magnitude of variation at a given frequency during each phase: summer and winter. This function processes data as samples s^{-1}, so for eight measurements in a day (every 3 hours), a sampling rate of 9.26×10^{-5} samples $s^{-}1$ was applied with a frequency of d^{-1} (Miller et al. 2021). A Hamming window was used for sidelobe trimming of the analyses, and the mean value for each parameter was subtracted in order to examine only the variation around the mean. Residual noise around a frequency of 0 was muted by applying a Butterworth high-pass filter with an order of 3 and cut off frequency at 1.0×10^{-5} (Miller et al. 2021). If two of the analyzed variables exhibit the same predominant frequency, their variation is assumed to be correlated regardless of direction and magnitude. Previous PSD analyses with similar parameters are considerably noisy below ~ 50 dB Hz^{-1}, making this value a cutoff threshold for this study. A 7-day moving average was applied to the pH time-series at both sites. All statistical analyses were conducted using Matlab (v2020a). All time-series reported in UTC.

Results

Annual time-series analysis

HOM and SEL sites both displayed seasonality in each measurement variable (Figures 5, 6). From July 2018 to August 2019, the mean pH at HOM was 7.93 ± 0.14, mean temperature was 7.17 ± 2.7°C, average salinity was 30.4 ± 0.94, and oxygen concentration 9.39 ± 0.7 mg/L. During the same period at SEL, the mean pH was 7.98 ± 0.13, mean temperature was 7.74 ± 1.97°C, salinity yielded an average of 31.01 ± 0.5, and mean oxygen concentration was 9.36 ± 0.79 mg/L (Table 1). HOM and SEL were significantly different with respect to all measurement variables, with P-Value < 0.0001 for all parameters except for oxygen concentration, where P-Value = 0.016.

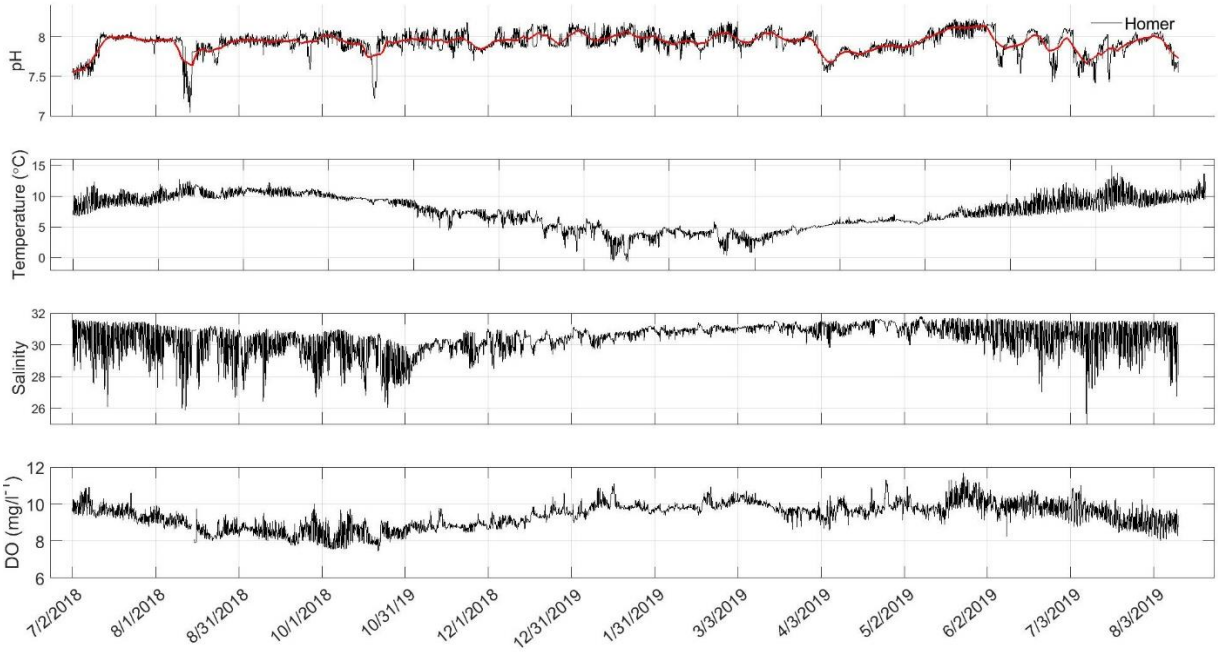

Figure 5. Homer time-series of pH, temperature, salinity, and dissolved oxygen for the entire deployment period, 7/2/18 to 8/4/2019. The red line in the upper panel (pH) denotes a 7-day moving average.

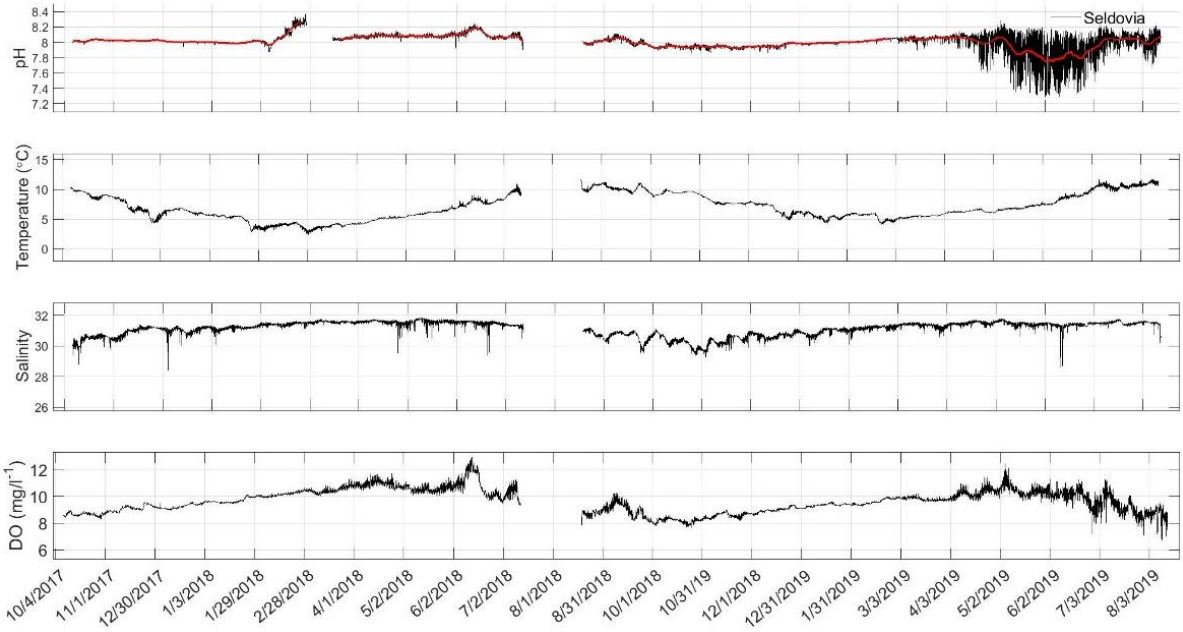

Figure 6. Seldovia time-series of pH, temperature, salinity, and dissolved oxygen for the entire deployment period, 10/7/17 to 8/4/2019. The red line in the upper panel (pH) denotes a 7-day moving average.

Table 1. Summary statistics of measured parameters, 7/2/2018 – 8/2/2019.

Variable	Mean	SE Mean	StDev	Min	Q1	Median	Q3	Max
HOM								
pH	7.93	0.00	0.14	7.22	7.87	7.94	8.03	8.22
Temperature (°C)	7.17	0.05	2.65	-0.65	5.10	7.13	9.53	14.91
Salinity	30.42	0.02	0.94	24.62	30.01	30.66	31.08	31.80
Oxygen (mg/L)	9.39	0.01	0.71	7.48	8.85	9.52	9.88	11.68
SEL								
pH	7.98	0.00	0.13	7.29	7.95	8.00	8.05	8.28
Temperature (°C)	7.74	0.04	1.97	4.14	5.97	7.52	9.60	11.77
Salinity	31.01	0.01	0.50	28.60	30.68	31.15	31.42	31.79
Oxygen (mg/L)	9.36	0.01	0.79	6.76	8.74	9.36	9.91	12.45

Seasonal time-series analysis

During the summer months, there was a weak positive relationship between pH and salinity (r^2 = 0.07) at HOM, indicating that changes in salinity had little influence over pH dynamics. The relationship between pH and oxygen concentrations was slightly stronger (r^2 = 0.11). Temperature had the strongest negative effect on pH (r^2 = 0.17). The temperature-salinity relationship at HOM was notable (r^2 = 0.67; Figure 7). Summertime pH dynamics at SEL appeared to only be slightly positively influenced by temperature (r^2 = 0.18), counter to what thermodynamics would predict, Salinity and oxygen had no effect on pH dynamics in SEL during summer. There was a weak relationship between temperature and salinity at SEL during summer (r^2 = 0.09; Figure 8).

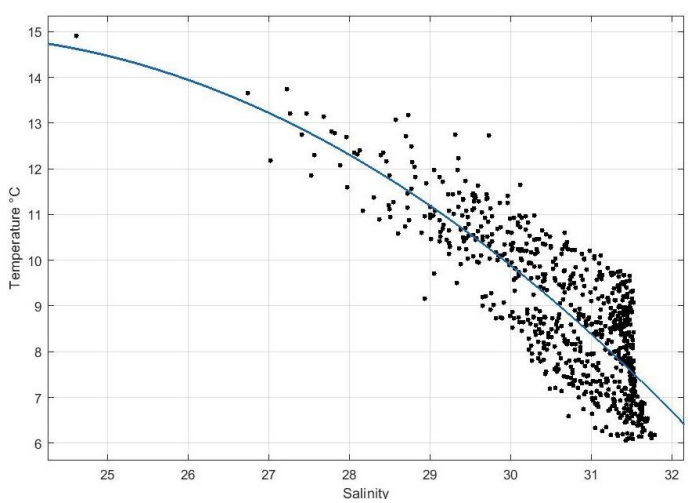

Figure 7. Homer summertime temperature-salinity scatterplot with a quadratic fit line (2nd order polynomial), r^2 = 0.67.

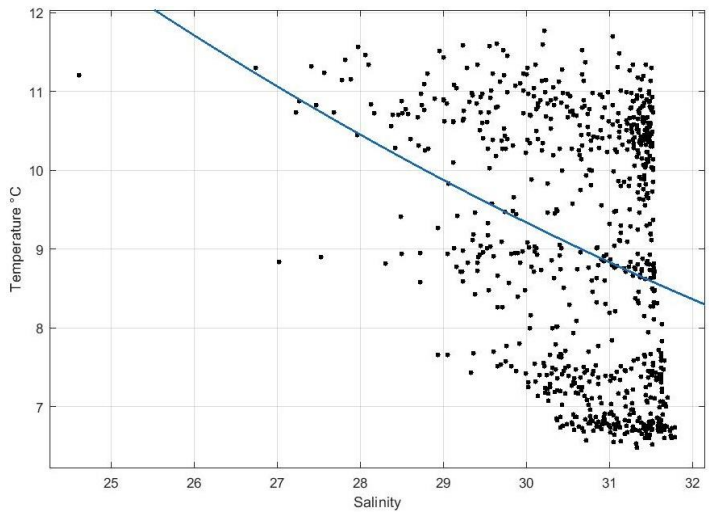

Figure 8. Seldovia summertime temperature-salinity scatterplot with a quadratic fit line (2nd order polynomial), $r^2 = 0.09$.

In general, at both sites, wintertime pH dynamics were attenuated compared to summer, and at HOM, only oxygen concentration was correlated with pH variability ($r^2 = 0.06$). However, SEL wintertime pH variability was strongly modulated by both biological metabolism and temperature as demonstrated by positive correlations of oxygen and pH ($r^2 = 0.35$) and temperature and pH ($r^2 = 0.40$). There was no relationship between salinity and pH in SEL during the winter months. The wintertime temperature-salinity relationship at SEL was positive ($r^2 = 0.35$), and evidence of three distinct water masses are visualized in Figure 9. At HOM, the distinct water masses are still present, however, less constrained (Figure 10), and there is a weak relationship between temperature and salinity ($r^2 = 0.06$). Overall, the relationships between pH dynamics and the other oceanographic variables were low, revealing the complex nature of nearshore processes.

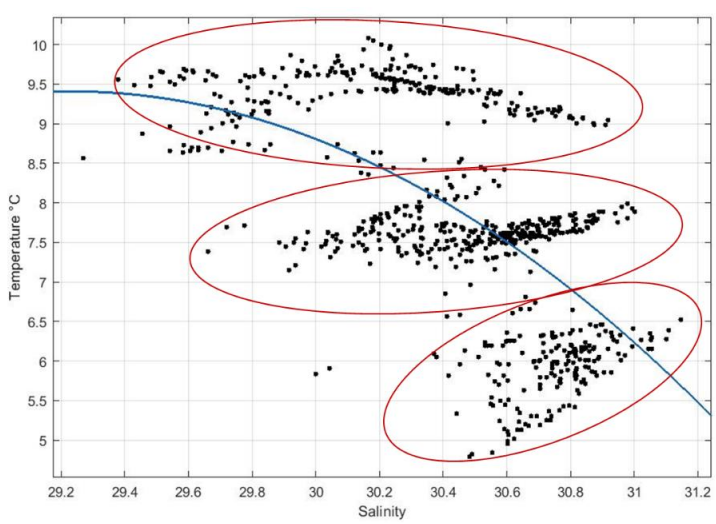

Figure 9. Scatterplot of temperature and salinity at Seldovia during wintertime. The red circles denote distinct water masses.

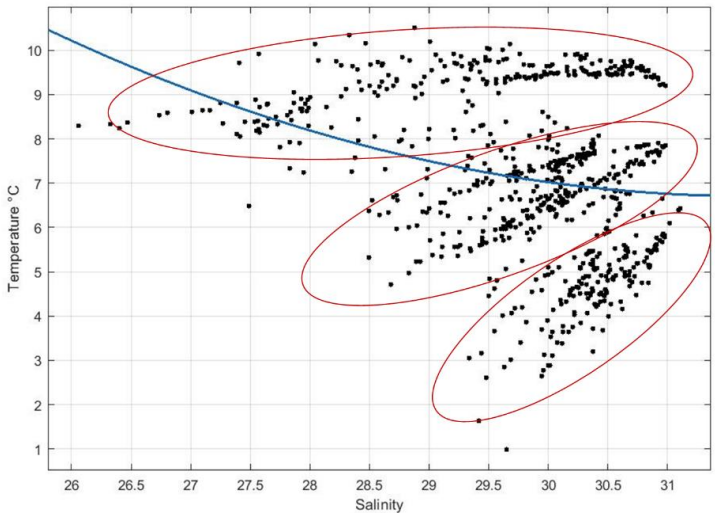

Figure 10. Scatterplot of temperature and salinity at Homer during wintertime. The red circles denote distinct water masses.

Power spectral density analysis

The frequency of pH variability was investigated to determine whether factors such as tide, photosynthesis, and other oceanographic processes that operate in the time domain impacted pH dynamics. The PSD of pH at HOM displayed several peaks (Figure 11), with the largest at 2 d^{-1}, indicating that tide played the greatest role in modulating pH. Peaks at 0.5 d^{-1} and 1 d^{-1} indicate that processes occurring once a day and once every two days also took place. The peak at 1 d^{-1} may indicate photosynthesis on a diel pattern influences pH daily. PSD at SEL had fewer peaks (Figure 12); the peaks at 2 and 4 d^{-1} indicate that the mixed semi-diurnal tide strongly influenced pH dynamics.

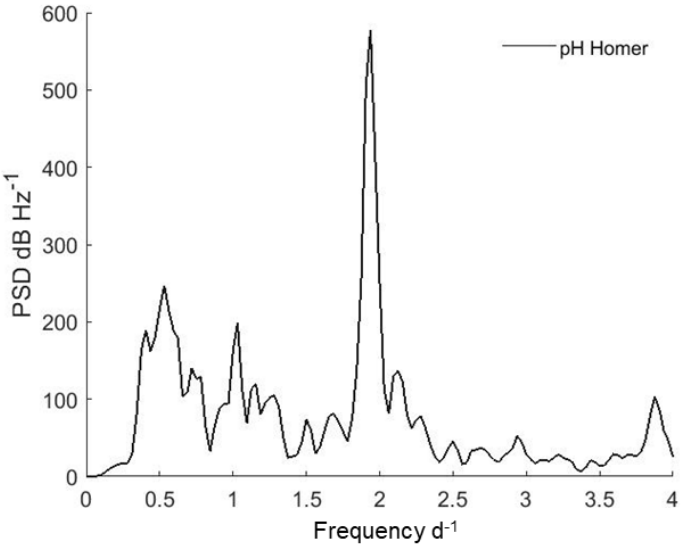

Figure 11. Homer summer Power Spectral Density (PSD) plot. The height of the spectra corresponds to the magnitude of pH at a given frequency.

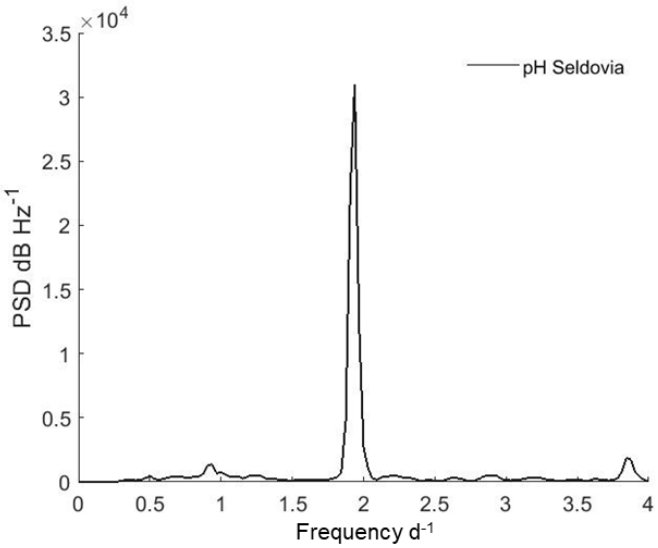

Figure 12. Seldovia summer Power Spectral Density (PSD) plot. The height of the spectra corresponds to the magnitude of pH at a given frequency.

Uncertainty estimates

Over the year-long deployment period, three reference samples were collected to determine the overall uncertainty of the pH time-series at HOM, occurring 00:00 8/15/18, 18:00 3/12/19, and 18:00 5/30/19. The mean uncertainty for HOM was 0.04 pH units. At SEL, reference samples were collected 21:00 12/14/18, 00:00 3/13/19, and 00:00 8/16/19. The SeaFET instrument was recalibrated 00:00 6/6/18; therefore, the seawater sample was used as a calibration point rather than a reference point. The total estimated uncertainty for the SEL pH time-series was 0.07 pH units.

Discussion

The results of this study yielded several distinct patterns. When comparing the annual time-series, HOM was more acidic, fresher, colder, and more stochastic in nature than SEL. The Student's T-test determined significant differences between the sites across all measurement variables. Mean annual pH at HOM was 0.04 pH units lower than SEL. Both sites had a range of 1 pH unit range during the study period. There was a difference in mean salinity with HOM 0.6 units lower than SEL, and on average, HOM was 0.6°C cooler than SEL. Temperature and salinity at HOM were impacted by freshwater from glaciers and the Fox River that enter the bay's head and exit at the Homer spit. Although they appear similar, mean oxygen concentrations were statistically significantly different. The minimum temperature at HOM reached -0.65°C, while the SEL minimum was 4.14°C, a four-degree difference. HOM also had the highest temperature recorded, 14.91°C, three degrees warmer than SEL. The total range of temperature at HOM was double that of SEL, at 15.56°C. Minimum salinity at HOM was four units lower than at SEL, and the maximum value for each site was identical at 31.8. Minimum oxygen concentration at SEL, 6.76 mg/L, was roughly 0.72 mg/L lower than HOM.

Detangling drivers of nearshore pH dynamics can be complex, as many factors either work in concert to increase pH amplitude or counteract each other to attenuate the pH signal. Both sites clearly experience seasonal patterns of all observed parameters, with steady summertime increases in temperature and periodic changes to salinity resulting from freshwater input from glacial melt and terrestrial sources. Oxygen concentration rose steadily at both sites from early spring through summer, with concentrations decreasing in fall. The short-term pH variability at HOM was present year-round, while SEL saw steady wintertime pH punctuated by increased amplitude during summer.

Summertime pH dynamics at HOM were weakly influenced by salinity, temperature, and oxygen. Although salinity was quite variable during the sample period, the concomitant changes in pH were negligible. Given the relationship between carbonate ion concentration and salinity, this result was somewhat surprising. Typical carbonate system responses to changes in salinity result in a reduction of pH due to dilution of carbonate ion concentration (Gonski et al. 2018). The HOM results are similar to those reported for Jakolof Bay (see Miller and Kelley 2021); however, the salinity variability at HOM is much greater than at Jakolof Bay. Biological metabolism, likely photosynthesis from phytoplankton, was modestly responsible for the fluctuation in pH. Temperature appeared to have the greatest influence over pH; as the temperature at HOM increased, the pH decreased. The strong temperature-salinity relationship demonstrates that source water from Cook Inlet was diluted with freshwater runoff entering KB rather than evidence of two distinct water masses. The drivers of pH variability were harder to detect at SEL. Temperature was positively correlated with pH; however, this result is counter to the laws of thermodynamics and is likely a result of biological metabolism, which covaried with rising and falling temperature on a diel timescale. SEL had no temperature-salinity relationship, as salinity varied little despite daily fluctuations in temperature.

Analysis of wintertime dynamics revealed markedly different patterns at each site compared with summertime values. Wintertime HOM pH was not strongly correlated with any other oceanographic variable. However, SEL exhibited clear drivers of pH dynamics. Temperature and oxygen concentrations were moderately correlated with high-frequency pH variability. At SEL, salinity variability in winter is greatly reduced and, thus, was not a factor in pH variability, perhaps elucidating the influence the other variables had on pH. Photosynthetic processes are muted during winter because of limited photosynthetically active radiation; however, organismal metabolism still occurs and can strongly influence pH. One of the most striking results of this study was the observation of water mass movement during the winter months. Upwelled water from the GoA can enter outer KB and circulate throughout before exiting at Homer Spit. Distinct water masses of differing densities infiltrated the bay (Figure 9) and were diluted with freshwater before exiting (Figure 10). The impact of high temperature and salinity variability due to solar warming and increased runoff have an inhibitory effect on detecting water mass movement during summer.

KB experiences a tidal range of ~ 4–5 m, one of the largest tidal ranges in the US, which undoubtedly governs pH dynamics throughout the bay. PSD frequency analysis of both sites during summer was generally similar, with peaks corresponding to 1, 2, and 4 d^{-1}, signaling a strong tidal influence on pH within the bay. Biological biomass and activity can influence pH dynamics and were likely factors that determined the relative differences between sites. HOM had less signal to noise when compared with SEL, an artifact of the lack of organismal biomass and extreme currents at HOM.

Conclusion

This study was the first to identify annual high-frequency pH variability in an Alaska BOEM OCS region. The chemical seascape links biological, physical, and chemical processes and is crucial to identifying the primary drivers of acidification in high-latitude coastal regions. The strongest drivers of pH dynamics in KB were tidal oscillation, followed by biological activity. Seasonal patterns also dominated, as winter and summer dynamics differed considerably. Characterizing regional high-frequency pH variability is essential in informing studies that determine the vulnerability of marine species to ocean acidification. This study highlights the need to include pH dynamics that vary with the tide on a diel timescale. KB is home to the largest oyster aquaculture production in the state, and the information gathered here is vital to determining the adaptive capacity of communities that rely on healthy marine ecosystems. It is unknown if the same processes similarly influence pH dynamics in larger Cook Inlet, and additional inquiry is needed to determine the factors that contribute to nearshore carbonate chemistry variability in other key BOEM regions.

Acknowledgments

I am very grateful to all the staff at the Kasitsna Bay lab, including Kris Holderied, Hans Pedersen, Connie Geagel, and Mike Geagal. I would also like to thank the undergraduate and graduate students who assisted with every aspect of this project, including Cale Miller, Noah Khalsa, Alta Dean, Ryan Kramer, Marina Washburn, Shelby Bacus, and Liza Hasan.

Study products

Results from this study were presented at the Kachemak Bay Science Conference 2018, Alaska Marine Science Symposium 2019, KBNERRS Islands and Ocean Sciences Lecture Series 2020, UAF College of Fisheries and Ocean Sciences Seminar Series 2020, and the Coastal Marine Institute Annual research Reviews in 2019 and 2020. A project-related manuscript titled "Seasonality and biological forcing modify the diel frequency of nearshore pH extremes in a sub-arctic Alaskan estuary" was accepted for publication in December 2020.

References

Bates NR, Mathis JT, Cooper LW (2009) Ocean acidification and biologically induced seasonality of carbonate mineral saturation states in the western Arctic Ocean. Journal of Geophysical Research: Oceans (114) C111 doi:org/10.1029/2008JC004862

Bresnahan PJ, Martz TR, Takeshita Y, Johnson KS, LaShomb M (2014) Best practices for autonomous measurement of seawater pH with the Honeywell Durafet. Methods in Oceanography 9: 44–60

Cavole LM, Demko AM, Diner RE, Giddings A, Koester I, Pagniello CMLS, Paulsen M-L, Ramirez-Valdez A, Schwenck SM, Yen NK, Zill ME, Franks PJS (2016) Biological Impacts of the 2013–2015 Warm-Water Anomaly in the Northeast Pacific: Winners, Losers, and the Future. Oceanography 29: 273–285

Cooney RT, Allen J, Bishop M, Eslinger D, Kline T, Norcross B, McRoy C, Milton J, Olsen J, Patrick V (2001) Ecosystem controls of juvenile pink salmon (*Onchorynchus gorbuscha*) and Pacific herring (*Clupea pallasi)* populations in Prince William Sound, Alaska. Fisheries Oceanography 10: 1–13

Dickson AG, Sabine CL, Christian JR, eds. (2007) Guide to best practices for ocean CO_2 measurements. PICES Special Publication 3, 191 pp.

Doney SC, Fabry VJ, Feely RA, Kleypas JA (2009) Ocean acidification: the other CO_2 problem. Annual Review of Marine Science 1: 169–192

Douglas N, Byrne R (2017) Achieving accurate spectrophotometric pH measurements using unpurified meta-cresol purple. Marine Chemistry 190: 66–72

Ekstrom JA, Suatoni L, Cooley SR, Pendleton LH, Waldbusser GG, Cinner JE, Ritter J, Langdon C, Van Hooidonk R, Gledhill D (2015) Vulnerability and adaptation of US shellfisheries to ocean acidification. Nature Climate Change 5: 207–214

Evans W, Mathis J, Cross J (2014) Calcium carbonate corrosivity in an Alaskan inland sea. Biogeosciences 11: 365–379

Evans W, Mathis JT, Ramsay J, Hetrick J (2015) On the frontline: tracking ocean acidification in an Alaskan shellfish hatchery. PloS One 10: e0130384

Evans W, Mathis JT, Winsor P, Statscewich H, Whitledge TE (2013) A regression modeling approach for studying carbonate system variability in the northern Gulf of Alaska. Journal of Geophysical Research: Oceans 118: 476–489 doi:10.1029/2012jc008246

Fabry VJ, McClintock JB, Mathis JT, Grebmeier JM (2009) Ocean acidification at high latitudes: the bellwether. Oceanography 22: 160

Gonski SF, Cai W-J, Ullman WJ, Joesoef A, Main CR, Pettay DT, Martz TR (2018) Assessment of the suitability of Durafet-based sensors for pH measurement in dynamic estuarine environments. Estuarine, Coastal and Shelf Science 200: 152–168

Hogan CM (2011) Gulf of Alaska. In: Cleveland CJ, ed., Encyclopedia of Earth. National Council for Science and the Environment. available at https://editors.eol.org/eoearth/wiki/Gulf_of_Alaska

Iken K, Konar B, Benedetti-Cecchi L, Cruz-Motta JJ, Knowlton A, Pohle G, Mead A, Miloslavich P, Wong M, Trott T (2010) Large-scale spatial distribution patterns of echinoderms in nearshore rocky habitats. PloS One 5: e13845

IPCC, International Panel on Climate Change (2013) Climate change 2013: the physical science basis: Working Group I contribution to the Fifth Assessment Report of the IPCC. Cambridge University Press, Cambridge United Kingdom and New York, New York.

Kapsenberg L, Hofmann G (2016) Ocean pH time-series and drivers of variability along the northern Channel Islands, California, USA. Limnology and Oceanography (61)3: 953–968 doi:10.1002/lno.10264

Kapsenberg L, Kelley AL, Shaw EC, Martz TR, Hofmann GE (2015) Near-shore Antarctic pH variability has implications for the design of ocean acidification experiments. Scientific Reports 5: 1–10

Konar B, Iken K, Cruz-Motta JJ, Benedetti-Cecchi L, Knowlton A, Pohle G, Miloslavich P, Edwards M, Trott T, Kimani E (2010) Current patterns of macroalgal diversity and biomass in northern hemisphere rocky shores. PloS One 5: e13195

Kroeker KJ, Micheli F, Gambi MC (2013) Ocean acidification causes ecosystem shifts via altered competitive interactions. Nature Climate Change 3: 156–159

Litzow MA, Hunsicker ME, Ward EJ, Anderson SC, Gao J, Zador SG, Batten S, Dressel SC, Duffy-Anderson J, Fergusson E (2020) Evaluating ecosystem change as Gulf of Alaska temperature exceeds the limits of preindustrial variability. Progress in Oceanography 186 doi:10.1016/j.pocean.2020.102393

Martz TR, Connery JG, Johnson KS (2010) Testing the Honeywell Durafet® for seawater pH applications. Limnology and Oceanography: Methods 8: 172–184

Mathis J, Cooley S, Lucey N, Colt S, Ekstrom J, Hurst T, Hauri C, Evans W, Cross J, Feely R (2014) Ocean acidification risk assessment for Alaska's fishery sector. Progress in Oceanography 136: 71–91 doi:1016/j.pocean.2014.07.001

Miller CA, Bonsell C, McTigue ND, Kelley AL (2021a) The seasonal phases of an Arctic lagoon reveal the discontinuities of pH variability and CO_2 flux at the air–sea interface. Biogeosciences, 18, 1203–1221 https://doi.org/10.5194/bg-18-1203-2021

Miller CA, Kelley A (2021) Seasonality and biological forcing modify the diel frequency of nearshore pH extremes in a subarctic Alaskan estuary. Limnology and Oceanography https://doi.org/10.1002/lno.11698

Miller CA, Pocock K, Evans W, Kelley AL (2018) An evaluation of the performance of Sea-Bird Scientific's SeaFET™ autonomous pH sensor: considerations for the broader oceanographic community. Ocean Science 14: 751–768

Miloslavich P, Cruz-Motta JJ, Klein E, Iken K, Weinberger V, Konar B, Trott T, Pohle G, Bigatti G, Benedetti-Cecchi L (2013) Large-scale spatial distribution patterns of gastropod assemblages in rocky shores. PLoS One 8: e71396

Neher TDH, Rosenberger AE, Zimmerman CE, Walker CM, Baird SJ (2014) Use of glacier river-fed estuary channels by juvenile Coho Salmon: transitional or rearing habitats? Environmental Biology of Fishes 97: 839–850

Pohle G, Iken K, Clarke KR, Trott T, Konar B, Cruz-Motta JJ, Wong M, Benedetti-Cecchi L, Mead A, Miloslavich P (2011) Aspects of benthic decapod diversity and distribution from rocky nearshore habitat at geographically widely dispersed sites. PloS One 6: e18606

Reisdorph SC, Mathis JT (2015) Assessing net community production in a glaciated Alaskan fjord. Biogeosciences 12: 5185–5198

Reisdorph SC, Mathis JT (2014) The dynamic controls on carbonate mineral saturation states and ocean acidification in a glacially dominated estuary. Estuarine, Coastal and Shelf Science 144: 8–18

Somero GN, Beers JM, Chan F, Hill TM, Klinger T, Litvin SY (2016) What changes in the carbonate system, oxygen, and temperature portend for the Northeastern Pacific Ocean: a physiological perspective. BioScience 66: 14–26

Waldbusser GG, Hales B, Langdon CJ, Haley BA, Schrader P, Brunner EL, Gray MW, Miller CA, Gimenez I, Hutchinson G (2015) Ocean acidification has multiple modes of action on bivalve larvae. PloS One 10: e0128376

Waldeck P, Larsson K (2013) Effects of winter water temperature on mass loss in Baltic blue mussels: implications for foraging sea ducks. Journal of Experimental Marine Biology and Ecology 444: 24–30

Walsh JE, Thoman RL, Bhatt US, Bieniek PA, Brettschneider B, Brubaker M, Danielson S, Lader R, Fetterer F, Holderied K (2018) The high latitude marine heat wave of 2016 and its impacts on Alaska. Bulletin of the American Meteorological Society 99: S39–S39

Waters CN, Zalasiewicz J, Summerhayes C, Barnosky AD, Poirier C, Gałuszka A, Cearreta A, Edgeworth M, Ellis EC, Ellis M, Jeandel C, Leinfelder R, McNeill JR, Richter Dd, Steffen W, Syvitski J, Vidas D, Wagreich M, Williams M, Zhisheng A, Grinevald J, Odada E, Oreskes N, Wolfe AP (2016) The Anthropocene is functionally and stratigraphically distinct from the Holocene. Science 351 doi:10.1126/science.aad2622

The Department of the Interior Mission

As the Nation's principal conservation agency, the Department of the Interior has responsibility for most of our nationally owned public lands and natural resources. This includes fostering the sound use of our land and water resources, protecting our fish, wildlife and biological diversity; preserving the environmental and cultural values of our national parks and historical places; and providing for the enjoyment of life through outdoor recreation. The Department assesses our energy and mineral resources and works to ensure that their development is in the best interests of all our people by encouraging stewardship and citizen participation in their care. The Department also has a major responsibility for American Indian reservation communities and for people who live in island communities.

The Bureau of Ocean Energy Management

The Bureau of Ocean Energy Management (BOEM) works to manage the exploration and development of the nation's offshore resources in a way that appropriately balances economic development, energy independence, and environmental protection through oil and gas leases, renewable energy development and environmental reviews and studies.